HHS Public Access

Author manuscript

Brain Stimul. Author manuscript; available in PMC 2024 March 18.

Published in final edited form as:

Brain Stimul. 2023 ; 16(6): 1764–1775. doi:10.1016/j.brs.2023.11.016.

Oscillatory network markers of subcallosal cingulate deep brain stimulation for depression

M. Scherer[a,b,1], **I.E. Harmsen**[a,c,d,1], **N. Samuel**[a,c], **G.J.B. Elias**[a,c], **J. Germann**[a,c], **A. Boutet**[a,e], **C.E. MacLeod**[f], **P. Giacobbe**[g], **N.C. Rowland**[h,i], **A.M. Lozano**[a,c,j,2], **L. Milosevic**[a,b,j,k,2,*]

[a]Krembil Brain Institute, University Health Network, Toronto, Canada

[b]Institute of Biomedical Engineering, University of Toronto, Canada

[c]Division of Neurosurgery, Department of Surgery, Toronto Western Hospital, University of Toronto, Toronto, Ontario, Canada

[d]Mitchell Goldhar MEG Unit, University Health Network, Toronto, Canada

[e]Joint Department of Medical Imaging, University of Toronto, Canada

[f]Department of Psychology, Neuroscience & Behaviour, McMaster University, Hamilton, Ontario, Canada

[g]Department of Psychiatry, Sunnybrook Health Sciences, University of Toronto, Toronto, Ontario, Canada

[h]Department of Neurosurgery, Medical University of South Carolina, Charleston, SC, USA

[i]Murray Center for Research on Parkinson's Disease and Related Disorders, Medical University of South Carolina, Charleston, SC, USA

[j]Center for Advancing Neurotechnological Innovation to Application (CRANIA), Toronto, Canada

[k]KITE Research Institute, University Health Network, Toronto, Canada

Abstract

[*]Corresponding author. 399 Bathurst St. 11MP301, Toronto, ON, M5T 2S6, Canada. luka.milosevic@mail.utoronto.ca (L. Milosevic).
[1]These authors contributed equally.
[2]These senior authors contributed equally.

CRediT authorship contribution statement

M. Scherer: Conceptualization, Methodology, Software, Validation, Formal analysis, Investigation, Resources, Data curation, Writing – original draft. **I.E. Harmsen:** Conceptualization, Methodology, Investigation, Data curation, Writing – original draft. **N. Samuel:** Resources, Writing – review & editing. **G.J.B. Elias:** Resources, Writing – review & editing. **J. Germann:** Resources, Writing – review & editing. **A. Boutet:** Writing – review & editing. **C.E. MacLeod:** Writing – review & editing. **P. Giacobbe:** Writing – review & editing. **N.C. Rowland:** Writing – review & editing. **A.M. Lozano:** Conceptualization, Methodology, Investigation, Resources, Project administration, Funding acquisition. **L. Milosevic:** Conceptualization, Methodology, Validation, Resources, Writing – original draft, Visualization, Supervision, Project administration, Funding acquisition.

Declaration of competing interest

All other authors declare no competing interests.

Appendix A. Supplementary data

Supplementary data to this article can be found online at https://doi.org/10.1016/j.brs.2023.11.016.

Identifying functional biomarkers related to treatment success can aid in expediting therapy optimization, as well as contribute to a better understanding of the neural mechanisms of the treatment-resistant depression (TRD) and subcallosal cingulate deep brain stimulation (SCC-DBS).

Magnetoencephalography data were obtained from 16 individuals with SCC-DBS for TRD and 25 healthy subjects. The first objective of the study was to identify region-specific oscillatory modulations that both (i) discriminate individuals with TRD (with SCC-DBS OFF) from healthy controls, and (ii) discriminate TRD treatment responders from non-responders (with SCC-DBS ON). The second objective of this work was to further explore the effects of stimulation intensity and frequency on oscillatory activity in the identified brain regions of interest.

Oscillatory power analyses led to the identification of brain regions that differentiated responders from non-responders based on modulations of increased alpha (8–12 Hz) and decreased gamma (32–116 Hz) power within nodes of the default mode, central executive, and somatomotor networks, Broca's area, and lingual gyrus. Within these nodes, it was also found that low stimulation frequency had stronger effects on oscillatory modulation than increased stimulation intensity.

The identified functional network biomarkers implicate modulation of TRD-related activity in brain regions involved in emotional control/processing, motor control, and the interaction between speech, vision, and memory, which have all been implicated in depression. These electrophysiological biomarkers have the potential to be used as functional proxies for therapy optimization. Additional stimulation parameter analyses revealed that oscillatory modulations can be strengthened by increasing stimulation intensity or reducing frequency, which may represent potential avenues of direction in non-responders.

Keywords

Deep brain stimulation; Magnetoencephalography; Treatment-resistant depression; Subcallosal cingulate; Alpha and gamma oscillations

1. Introduction

Clinical depression (major depressive disorder) affects a large portion of the global adult population annually [1], and up to one third of affected individuals are treatment-resistant [2]. Treatment-resistant depression (TRD) can be characterized by the insufficient response to conventional treatments, which typically entails the combination of antidepressant medication, psychotherapy, and electroconvulsive therapy [3]. As such, TRD represents a major social and economic burden worldwide (with affected individuals experiencing social and occupational dysfunction, and poor physical health, causing increased healthcare utilization), prompting research in the development of novel therapies for TRD.

Neuromodulation modalities, such as repetitive transcranial magnetic stimulation (rTMS), transcranial direct current stimulation (tDCS), and deep brain stimulation (DBS), are being researched as potential treatments for TRD. Of these interventions, DBS for TRD enables the direct stimulation of subcortical regions that cannot be targeted by non-invasive methods

and has the additional advantage that it may provide sustained therapeutic effects without the requirement of frequent clinical visits for therapy administration. DBS appears safe for TRD when targeting the subcallosal cingulate (SCC), medial forebrain bundle, or ventral capsule/striatum areas. However, data on the long-term efficacy of the treatment are highly variable. After two or more years of stimulation, the treatment response varied widely with striatal/capsular area DBS and with SCC-DBS [4–7].

While DBS efficacy can be quickly evaluated in people with Parkinson's disease or essential tremor due to the near instantaneous relief of motor symptoms [8], this does not apply to psychiatric disorders such as TRD. In this population, clinical evaluations are typically performed retrospectively using clinical assessment batteries which average mood over the course of weeks or months; hence the evaluation of multiple DBS configurations, the stimulation titration process, extends over months or years [9]. In addition to the immense time requirement, this process can also be subject to a high degree of external confounding influences (i.e., job loss, stress, etc.). Two contributors critically affecting outcome following the surgical implantation of the DBS leads are contact selection and stimulation programming. Given the high cost (in both patient well-being and healthcare resources) of qualitatively assessing the efficacy of a single stimulation configuration (contact selection and stimulation programming), appropriate early indicators of treatment success are strongly warranted by patients and healthcare professionals.

The first objective of this work was to use magnetoencephalography (MEG) to identify electrophysiological characteristics supportive in DBS lead placement confirmation and DBS contact selection, as MEG allows for high spatial resolution sampling of the underlying activity [10]. Therefore, we sought to identify functional biomarkers that could differentiate treatment responders from non-responders. As individually optimized settings are not yet established in new patients, this discriminative response profile would have to be inducible through generic, uniform stimulation parameters.

The second objective of this work was to gain a better mechanistic understanding of the impacts of stimulation intensity and frequency on the modulation of cortical network activity. Hence, we investigated the contrast of high versus low stimulation intensity (constraining frequency) and high versus low frequency (constraining intensity). In clinical settings, stimulation intensity is often titrated in accordance with side effect profiles [11]; however, investigations of frequency-dependence are of particular interest as many new experimental DBS indications default to the use of 130 Hz stimulation due to its success in movement disorders, rather than a comprehensive understanding of the functional implications.

2. Material and methods

2.1. Participants

People with TRD who had previously been implanted with bilateral SCC-DBS electrodes (n 16; Fig. 1A) were included in this study (details about surgical procedures are provided within the Supplementary Materials). Age- and sex-matched healthy controls (HC; n 25) without major neurological or psychiatric diseases were also recruited. All subjects provided

written informed consent. The study was approved by the University Health Network Research Ethics Board (Toronto, Canada) and was conducted in accordance with the Declaration of Helsinki. For people with TRD, disease severity was measured preoperatively and 12 months postoperatively by a psychiatrist (P.G.) using the 17-item Hamilton Depression Rating Scale (HAM-D17; Table 1). Seven patients were considered treatment responders (HAM-D17 change ≥50 %), and eight were considered non-responders. Clinical outcomes of patients 3, 6, 9, and 14 were reported in previous studies [12,13]. The patient's clinical details and therapeutic DBS settings are listed in Table 1. Additional clinical history data is available in Supplementary Table 1.

2.2. MEG recordings

The first objective of this study was to identify a network response profile that could differentiate responders from non-responders. MEG data (Elekta Neuromag TRIUX™, Helsinki, Finland; 306 channels each sampled at 1000 Hz; exemplary MEG signal, power spectrum, and spectrogram available as Supplementary Fig. 1) were acquired from HCs and people with TRD during DBS OFF and DBS ON (3 min per condition). MEG data were acquired in supine-positioned, eyes-closed, resting-state for patient comfort and data quality (i.e. reduced eye movements and blinking artifacts). In trials with DBS, stimulation was applied bilaterally at 130 Hz, 1.5 mA, 90 μs pulse width, bipolar 1–2+. Instead of using variable/patient-specific DBS parameters (see Table 1 for clinical DBS parameters), we used a unified DBS parameter set across all patients to establish a standardized approach for deriving a functional network response profile that may be predictive of therapeutic success in prospective contexts (i.e., when optimized clinical parameters are otherwise unknown in the early stages of therapy initiation).

The second objective of this study was to investigate how changes to stimulation settings may impact cortical network activity. To do this, three intensity/frequency combinations of stimulation were applied unilaterally in the left hemisphere: 1.5 mA & 130 Hz (baseline condition); 3.0 mA & 130 Hz (to study the effect of stimulation intensity); and 1.5 mA & 20 Hz (to study the effect of stimulation frequency).

For analyses, after digitally removing ambient artifacts (tSSS; Elekta Neuromag MaxFilter software version 2.2.12, Elekta, Helsinki, Finland; 10s windows; subspace correlation limit of 0.980), line noise (60 Hz; and its harmonics) and high-frequency components (>120 Hz), data were downsampled to 240 Hz. MEG data were then transformed from sensor to source space (depth bias correction via dSPM; for more details, see Supplementary Materials), transformed into fs-average space, and clustered within anatomical boundaries defined in the Desikan-Killiany atlas (Supplementary Fig. 2) [14]. Subsequently, DBS artifacts (and their harmonics) were notch filtered. Using representative sub-bands, cluster-wise spectral power was calculated via Welch's method for delta (2–4 Hz), theta (4–8 Hz), alpha (8–12 Hz), beta (12–32 Hz), gamma (32–116 Hz), and broadband (2–116 Hz) frequencies. Power within a given sub-band was normalized with respect to broadband (2–116 Hz) power to produce relative power values. Additional methodological details regarding source reconstruction and data processing are available in Supplementary Materials.

2.3. Statistics

Effects were quantified using linear mixed models (Python-FiNNPy [15]/R-lme4 [16]). For the first objective of this work (identifying network-level functional biomarkers of treatment response) a cortical region was considered to be a region of interest (ROI) if both of the following statistical criteria were satisfied: (1) a statistically significant oscillatory difference was identified in people with TRD (responders and non-responders with SCC-DBS OFF) compared to HC, which was (2) counteracted by SCC-DBS in responders only ("compensation" to a level no longer statistically significantly different from HC, or "overcompensated" such that the effect was statistically significant but in the opposite direction to the TRD-related effect). For each ROI, correlations were also performed between relative changes in spectral power and clinical benefit; however, no regions found to exhibit a significant correlation (Supplementary Figs. 3 and 4). For the second objective of this work (investigating the effects of changing stimulation settings), we applied the same statistical criteria at regions of interest identified as in the first part of the analysis.

The validity and reliability of all observations were confirmed using both 15-s and 30-s windows for data epoching. Since the multi-layered statistical approach necessitates a feature to be significant across three different hypotheses times two epoch window sizes, a high threshold for statistical significance was enforced, and no further correction methods were employed. Statistical significance was set at $p < 0.05$. Detailed statistical values are available in Supplementary Table 2.

2.4. Data availability

The study data may be shared upon reasonable request to the corresponding author.

3. Results

Resting-state magnetoencephalography (MEG) recordings were acquired from people with TRD (n 16) during SCC-DBS OFF and ON and from HCs (n 25). The characteristics of the TRD study participants are presented in Table 1. HCs comprised 12 males and 13 females, with an average age of 38.1 ± 3.9 years. There were no significant differences between HC and TRD group means for age ($p = 0.179$, $t [38] = -1.37$) or sex ($p = 0.462$, $\chi 2 [2,40] = 0.54$).

Spatially, all identified ROIs were located within the left hemisphere, except for the right paracentral lobule; spectrally, the identified effects were limited to compensation of increased alpha band (8–12 Hz) power as well as compensation and overcompensation of decreased gamma (32–116 Hz) power (summarized in Fig. 1B).

3.1. Responder-specific compensation of increased alpha band power

In several cortical regions, we identified responder-specific compensation of TRD-related increased alpha band (8–12 Hz) power (Fig. 2). Compared to HCs, TRD patients with SCC-DBS OFF had increased alpha activity, which was reduced to levels comparable to HCs in responders only when SCC-DBS was turned ON. This alpha compensation occurred

in the left retrosplenial cortex, inferior frontal cortex pars triangularis, postcentral gyrus, precentral gyrus, supramarginal gyrus, and the right paracentral lobule.

3.2. Responder-specific compensation of decreased gamma band power

We also identified responder-specific compensation of TRD-related decreased gamma band (32–116 Hz) power (Fig. 3). Compared to HCs, TRD patients with SCC-DBS OFF had decreased gamma activity, which was increased to levels comparable to HCs in responders only when SCC-DBS was turned ON. This gamma compensation occurred in the left posterior cingulate, paracentral lobule, rostral middle frontal cortex (containing the dorsolateral prefrontal cortex; Fig. 3C), lingual gyrus, inferior frontal cortex pars opercularis, and the inferior frontal cortex pars triangularis.

3.3. Responder-specific overcompensation of decreased gamma band power

Lastly, we identified responder-specific overcompensation of TRD-related decreased gamma band (32–116 Hz) power (Fig. 4). Compared to HCs, TRD patients with SCC-DBS OFF had decreased gamma activity, which was increased beyond levels observed in HCs in responders only when SCC-DBS was turned ON. This gamma overcompensation occurred in the left retrosplenial cortex, precentral gyrus, supramarginal gyrus, postcentral gyrus, caudal middle frontal gyrus, and the banks of the superior temporal sulcus.

3.4. Investigation of the effects of stimulation intensity and frequency

To determine the modulatory effects of stimulation amplitude and frequency on cortical activity, we compared different DBS settings on oscillatory activity in the previously identified ROIs. Firstly, unilateral stimulation had weaker modulatory effects than bilateral stimulation in the alpha and gamma frequency bands. Bilateral stimulation at 130 Hz and 1.5 mA was associated with undercompensated activity (i.e., DBS-related changes to TRD-related activity in the direction of compensation; but activity levels remain statistically significantly different from HCs) in non-responders and compensated or overcompensated activity in responders (Fig. 5A; summary of results presented in Figs. 2–4). In contrast, unilateral stimulation was associated with undercompensated activity in non-responders and responders (Fig. 5B).

Cortical modulatory effects were more substantial when DBS intensity was increased. When unilateral stimulation at 130 Hz was increased from 1.5 to 3.0 mA, modulatory effects were strengthened overall (i.e., less undercompensated nodes; Fig. 5C). In the alpha band, activity within all nodes became compensated in responders, while effects remained generally undercompensated in non-responders. In the gamma band, while activity within more nodes became compensated overall, this response was generally more often observed in non-responders. Statistical details for the cortical response to changes in stimulation amplitude are available in Supplementary Figs. 5 and 6.

Cortical modulatory effects were also more substantial when DBS frequency was decreased. When unilateral stimulation at 1.5 mA was decreased from 130 to 20 Hz, modulatory effects were strengthened overall (i.e., less undercompensated nodes and more overcompensated nodes; Fig. 5D). In the alpha and gamma bands, activity with nodes became compensated

or overcompensated in responders, whereas activity became compensated or remained undercompensated in non-responders. The strengthening of modulatory effects was greater with titrating stimulation frequency than amplitude. Statistical details for the cortical response to changes in stimulation frequency are available in Supplementary Figs. 5 and 6.

4. Discussion

Currently, deep brain stimulation (DBS) parameter optimization in people with treatment-resistant depression (TRD) is solely informed through subjective assessment tools (such as self-reports and clinician observations) and requires months of adjustment in order to determine optimal settings. Consequently, this strongly limits the number of DBS parameter combinations being trialed for TRD due to limited time and resources.

In this study, we lay the groundwork for this process to be augmented by the use of an objective measure, namely individualized electrophysiological feedback, to expedite the process. We identified electrophysiological profiles related to effective treatment responses, which may be used to aid in DBS lead placement/contact selection. The use of electrophysiological feedback to determine electrode placement has long been considered a gold-standard for DBS in for movement disorders [17], and more recently, specific electrophysiological profiles (e.g. beta frequency peaks) have been shown to align with the clinically most effective contacts [18], suggesting that electrophysiological information can be used to guide stimulation programming [19,20]. The electrophysiological profiles identified herein may be employed for such purposes, but in the context of TRD, to verify DBS lead placement and contact selection.

Various EEG-based biomarkers have previously been suggested to be indicative of response status in DBS for TRD. Some examples include increases in frontal theta cordance [21], decreases in frontal alpha and beta power [22], and right frontal theta and left parietal alpha power hemispheric asymmetries [23]. One potentially unique element of our methodological approach compared to previous studies was that ROI identification was based on DBS modulatory effects that were counter-directional to TRD-specific effects, thus identifying brain areas in which DBS shifted the electrophysiological profile of people with TRD towards one more reflective of healthy controls.

In addition to exploring biomarkers indicative of treatment response type, we also identified the electrophysiological responses associated with changes in SCC-DBS amplitude (1.5 mA vs. 3 mA) and frequency (20 Hz vs. 130 Hz). While low-frequency subthalamic stimulation (<50 Hz) is ineffective/disadvantageous in movement disorders [24], this may not necessarily extend to psychiatric disorders such as TRD. Given that low-frequency stimulation produced stronger network modulations herein, low-frequency stimulation may be a viable alternative in TRD, especially for those that do not benefit from high-frequency stimulation. The vastness of the potential search space for optimized settings for TRD further emphasizes the need of a timely way to assess a given DBS program's potential efficacy, which may be provided via rapidly assessable electrophysiological biomarkers.

In the context of this study, it was found that modulation of TRD-related activity in the default mode network (DMN), central executive network (CEN), and somatomotor network, as well as Broca's area, lingual gyrus, and temporal areas, could differentiate responders from non-responders. These regions are involved in emotional control and processing, motor control, and the interaction between speech, vision, and memory, which have all been implicated in depression [25–29]. The spectral characteristics of these observations, namely amplified low-frequency and decreased high-frequency (gamma) oscillations, mirror previous reports on TRD-specific changes [30]. As such, the following sections put our findings related to the neuromodulatory network effects of DBS in TRD into context with respect to well-established functional brain networks.

4.1. Modulated nodes in the default mode network

The DMN is, among other functions, involved in emotional processing [31] and has been implicated in depression, specifically TRD [32]. Several cortical regions that are part of the DMN network were identified in our study as nodes of interest, including the posterior cingulate cortex (PCC), retrosplenial cortex (RSC) [33], and supramarginal gyrus (SG) [34]. Triggered by emotionally linked cues, interactions between structures within the DMN have been observed during the processing of emotional experiences [35] and contextual learning in rodents [36]. In addition, the DMN plays a crucial role in memory formation and emotion-memory linkage. During resting periods, the network processes memory-related information in self-referential tasks such as introspection, worry, rumination [37], and other memory-related tasks (spatial and episodic) [38,39]. The RSC, in particular, is a node in the DMN that is anatomically well-situated to fuse emotions and memory [40] and has been implicated in fear conditioning [41] and contextual learning [36] in rodents. Furthermore, increased RSC low-frequency (4–12 Hz) and gamma activities have been associated with mnemonic functions [41]. Complementary evidence from human studies suggests RSC blood flow [42] and BOLD activity increase during emotional processing [43]. Increased RSC BOLD activity has also been linked to modulations in RSC alpha power [44]. Generally, RSC and PCC are commonly activated in emotion processing [40], as is the SG. The SG has also been shown to be activated in tasks related to emotion identification [45].

Furthermore, TRD-specific changes within the DMN have been linked to several psychiatric/neurological disorders such as Alzheimer's disease [46], major depression [28], obsessive-compulsive disorder [47], social phobia [48], and schizophrenia [49]. While metabolic activity in the RSC/PCC is decreased in Alzheimer's disease [46], it is increased in people with depression [50]. Additionally, increased depressive symptom severity has been associated with increased left RSC/PCC volume [51]. Similarly, cortical thickening has been observed in the SG of people with major depressive disorder [29]. Overall, the aforementioned studies support the potential importance of modulating certain TRD-relevant nodes of the DMN uncovered by this work, namely, responder-specific compensation of TRD-related increased alpha power (RSC and SG) and decreased gamma power (PCC).

4.2. Modulated nodes in the central executive network

The CEN is involved in attention control, working memory, and decision-making [52]. It primarily consists of the dorsolateral prefrontal cortex (dlPFC) and posterior parietal cortex (PPC) [53]. Although activity in the CEN is closely connected to the DMN, the two networks display anticorrelated behavior [54]. Gamma band activity in the CEN, particularly the dlPFC, has been connected with working memory performance [55]. Likewise, decreased gamma activity in the dlPFC has also been associated with reduced cognitive control and blunted reward learning in people with depression [56]. Reduced glucose metabolic rates have also been observed in the left dlPFC of people with depression symptoms [25]. These studies reflect our observation of TRD-related decreased gamma power in the left rostral middle frontal cortex (RMFC), which contains the left dlPFC. In particular, we found a responder-specific compensation of TRD-related decreased gamma band power in the left RMFC/dlPFC region with SCC-DBS. Similar results have been reported when applying transcranial magnetic stimulation (TMS) to the left dlPFC [57]. As such, the left dlPFC is a common target for TMS in depression treatment [58], likely due to its role in dopamine release [59] and its connections to several cortical and subcortical regions implicated in depression [60].

4.3. Modulated nodes of other networks

In responders, SCC-DBS was also associated with the modulation of other brain regions and networks that are functionally and structurally connected to the DMN and CEN. One such network that was implicated in our study was the somatomotor network (pre- and postcentral gyri) and surrounding areas (paracentral lobule). Indeed, TRD-specific alterations have previously been shown throughout this network in people with depression [61], such as increases in white matter hyperintensities [62]. These observations have often been linked to psychomotor retardation [62], a common symptom of depression [63]. Our study identified responder-specific compensation of increased alpha power (pre- and postcentral gyri and paracentral lobule) and decreased gamma power (paracentral lobule). Acute modulatory effects in these regions are likely mediated by *trans*-synaptic connectivity to SCC via the thalamus [64, 65].

We also observed responder-specific compensation of increased alpha power (pars triangularis) and decreased gamma power (pars triangularis and opercularis) within the inferior frontal cortex. Disease-related changes in altered anatomy have been reported in the pars opercularis [29] and triangularis [66] (forming Broca's area) in people with depression. Moreover, in people with depression, reduced oscillatory beta-band power was measured in the vicinity of Broca's area, relating to the error rates in phonological tasks [67]. Anatomically, these nodes within Broca's area are connected to the amygdala and are thought to play a role in a top-down control mechanism in worrying [68]. The amygdala, in turn, has reciprocal connections to the SCC, indirectly linking the nodes of Broca's area to the target of SCC-DBS.

We also identified responder-specific compensation of decreased gamma power in the lingual gyrus. This region is thought to play an important role in TRD-specific visual processing in people with depression [26]. Larger gray matter volumes of the lingual gyrus

have been associated with better performance in neuropsychological tests [26]. Functionally, activations of the lingual gyrus have been connected to activations of the amygdala [69].

Lastly, we observed responder-specific overcompensation of decreased gamma power in the left superior temporal sulcus and left caudal middle frontal gyrus. Changes to the superior temporal sulcus may be associated with sleep quality in depression [70].

4.4. Clinical utility of the identified functional network activation profile

Anatomically, the SCC (DBS target) encompasses the cingulum, forceps minor, and uncinate fasciculus bundles [71,72]. It has bidirectional structural connectivity with other brain regions, such as the orbitofrontal cortex [65], enabling remote DBS effects. Hence, responder-specific differences in cortical electrophysiology between people with TRD and HCs can manifest throughout various cortical regions. Similar to previously described MRI-based targeting strategies [72], the herein presented electrophysiological profile may be used as a marker for DBS lead placement and contact selection. DBS can be activated according to the standardized DBS parameters employed herein (1.5 V, 130 Hz), using a variety of contact pair combinations. The practitioner should seek to achieve the described responder-specific network activation profile (resembling the HC profile). The use of bipolar contact pairs would contain the (monopolar) DBS contact to be considered for clinical application, reducing the number of candidates from 4 to a maximum of 2 DBS contacts. The use of a standardized DBS parameter set, assuming no *a priori* knowledge of the eventual optimal stimulation parameters, allows for an application in prospective contexts. If and when the most appropriate contacts are selected based on the network response, settings can then be further modified on an individual basis to optimize the therapeutic window (i.e., increasing stimulation amplitude to a level just below the side effect threshold). If high-frequency stimulation is unable to achieve the desired network response, low-frequency stimulation can be considered, given the ability to produce stronger modulatory effects.

5. Limitations

This study applied SCC-DBS using a unified parameter set to identify functional biomarkers associated with treatment response in individuals with TRD. As such, patient-specific parameters determined clinically were not used in the study. Moreover, bipolar stimulation was employed to limit stimulation artifacts during MEG recordings. In addition, a unified stimulation amplitude was used to identify an electrophysiological profile that may be used to optimize treatment delivery in prospective contexts. This would otherwise not be possible if using heterogeneous stimulation settings. While this approach cannot be used to calibrate DBS amplitude per se, it provides a viable avenue for DBS lead position verification and contact selection. The analyses led to identifying a discriminative functional network profile derived from 3-min MEG recordings, which may be informative of responder status. However, the patient sample size was limited, and while oscillatory changes in identified ROIs could discriminate responders from non-responders, the degree of change in any given region was not found to be associated with the degree of benefit. As such, the potential clinical utility of the identified functional network profile would need to be established by obtaining MEG scans at an early stage in therapy initiation to guide DBS programming.

Additionally, although our results indicate that low-frequency SCC-DBS may have the strongest effects on TRD-related activity, clinical applicability is yet to be confirmed. Moreover, future mechanistic studies can consider the investigation of a greater range of frequencies and intensities than employed here. Furthermore, it is necessary to consider that TRD is a highly heterogeneous disorder with variable symptomatology and associated electrophysiological profiles, whereas our analysis is limited to a binary discretization of responder status due to the limited data in this retrospective study. Moreover, our interpretations of the presented findings are limited to the identified areas of interest and their reported relevance in TRD but do not provide an exhaustive overview of all potentially involved cortical regions, their functions, or TRD-specific alterations in TRD.

6. Conclusion

This study is among the first to use MEG to examine whole-brain and region-specific cortical responses to SCC-DBS in people with TRD. The application of SCC-DBS at unified parameter settings led to the identification of functional biomarkers that could differentiate responders from non-responders characterized by modulations of increased alpha and decreased gamma power in nodes of the DMN, CEN, and somatomotor network, as well as Broca's area and lingual gyrus – regions that have been implicated in behavioral functions and impairments associated with depression. The identified responder-specific profile may represent a functional readout that can be used for optimizing SCC-DBS therapy via improved candidate selection, surgical targeting, and DBS setting selection in prospective contexts. Furthermore, our interrogations of stimulation settings revealed that increasing stimulation amplitude or reducing frequency strengthened modulatory network effects.

Supplementary Material

Refer to Web version on PubMed Central for supplementary material.

Funding

This work was supported by the Alexander von Humboldt Foundation (M.S.), Canadian Institutes of Health Research (I.E.H.), National Institutes of Health Neurosurgeon Research Career Development Program K12 grant (N.C.R.), Canada Research Chair in Neuroscience (A.M. L.), and New Frontiers in Research Fund NFRFE-2021-00261 (L.M.).

A.M.L. is a consultant to Abbott, Boston Scientific, Medtronic, and Functional Neuromodulation. L.M. has received honoraria and travel funds from Medtronic (unrelated to this work).

References

[1]. Institute of Health Metrics and Evaluation. Global health data exchange (GHDx). n. d, http://ghdx.healthdata.org/gbd-results-tool?paramsgbd-api-2019-permalink/f8f71e9a6f2b3bbb36aa9f8e1d521c25. [Accessed 4 March 2023].

[2]. Kennedy SH, Giacobbe P. Treatment resistant depression— advances in somatic therapies. Ann Clin Psychiatr 2007;19:279–87. 10.3109/10401230701675222.

[3]. Al-Harbi KS. Treatment-resistant depression: therapeutic trends, challenges, and future directions. Patient Prefer Adherence 2012;6:369–88. 10.2147/PPA.S29716. [PubMed: 22654508]

[4]. Holtzheimer PE, Kelley ME, Gross RE, Filkowski MM, Garlow SJ, Barrocas A, et al. Subcallosal cingulate deep brain stimulation for treatment-resistant unipolar and bipolar depression. Arch Gen Psychiatr 2012;69:150–8. 10.1001/archgenpsychiatry.2011.1456. [PubMed: 22213770]

[5]. Holtzheimer PE, Husain MM, Lisanby SH, Taylor SF, Whitworth LA, McClintock S, et al. Subcallosal cingulate deep brain stimulation for treatment-resistant depression: a multisite, randomised, sham-controlled trial. Lancet Psychiatr 2017; 4:839–49. 10.1016/S2215-0366(17)30371-1.

[6]. Kennedy SH, Giacobbe P, Rizvi SJ, Placenza FM, Nishikawa Y, Mayberg HS, et al. Deep brain stimulation for treatment-resistant depression: follow-up after 3 to 6 years. Aust J Pharm 2011;168:502–10. 10.1176/appi.ajp.2010.10081187.

[7]. Merkl A, Aust S, Schneider G-H, Visser-Vandewalle V, Horn A, Kühn AA, et al. Deep brain stimulation of the subcallosal cingulate gyrus in patients with treatment-resistant depression: a double-blinded randomized controlled study and long-term follow-up in eight patients. J Affect Disord 2018;227:521–9. 10.1016/j.jad.2017.11.024. [PubMed: 29161674]

[8]. McIntyre CC, Anderson RW. Deep brain stimulation mechanisms: the control of network activity via neurochemistry modulation. J Neurochem 2016;139:338–45. 10.1111/jnc.13649. [PubMed: 27273305]

[9]. Dandekar MP, Fenoy AJ, Carvalho AF, Soares JC, Quevedo J. Deep brain stimulation for treatment-resistant depression: an integrative review of preclinical and clinical findings and translational implications. Mol Psychiatr 2018;23: 1094–112. 10.1038/mp.2018.2.

[10]. Illman M, Laaksonen K, Liljeström M, Jousmäki V, Piitulainen H, Forss N. Comparing MEG and EEG in detecting the ~20-Hz rhythm modulation to tactile and proprioceptive stimulation. Neuroimage 2020;215:116804. 10.1016/j.neuroimage.2020.116804.

[11]. Ramasubbu R, Lang S, Kiss ZHT. Dosing of electrical parameters in deep brain stimulation (DBS) for intractable depression: a review of clinical studies. Front Psychiatr 2018;9.

[12]. Lozano AM, Giacobbe P, Hamani C, Rizvi SJ, Kennedy SH, Kolivakis TT, et al. A multicenter pilot study of subcallosal cingulate area deep brain stimulation for treatment-resistant depression: clinical article. J Neurosurg 2012;116:315–22. 10.3171/2011.10.JNS102122. [PubMed: 22098195]

[13]. Lozano AM, Mayberg HS, Giacobbe P, Hamani C, Craddock RC, Kennedy SH. Subcallosal cingulate gyrus deep brain stimulation for treatment-resistant depression. Biol Psychiatr 2008;64:461–7. 10.1016/j.biopsych.2008.05.034.

[14]. Desikan RS, Ségonne F, Fischl B, Quinn BT, Dickerson BC, Blacker D, et al. An automated labeling system for subdividing the human cerebral cortex on MRI scans into gyral based regions of interest. Neuroimage 2006;31:968–80. 10.1016/j.neuroimage.2006.01.021. [PubMed: 16530430]

[15]. Scherer M, Wang T, Guggenberger R, Milosevic L, Gharabaghi A. FiNN: a toolbox for neurophysiological network analysis. Network Neuroscience 2022:1–34. 10.1162/netn_a_00265. [PubMed: 35350585]

[16]. Bates D, Mächler M, Bolker B, Walker S. Fitting linear mixed-effects models using lme4. J Stat Software 2015;67:1–48. 10.18637/jss.v067.i01.

[17]. Hutchison WD, Allan RJ, Opitz H, Levy R, Dostrovsky JO, Lang AE, et al. Neurophysiological identification of the subthalamic nucleus in surgery for Parkinson's disease. Ann Neurol 1998;44:622–8. 10.1002/ana.410440407. [PubMed: 9778260]

[18]. Milosevic L, Scherer M, Cebi I, Guggenberger R, Machetanz K, Naros G, et al. Online mapping with the deep brain stimulation lead: a novel targeting tool in Parkinson's disease. Mov Disord 2020;35:1574–86. 10.1002/mds.28093. [PubMed: 32424887]

[19]. Connolly MJ, Cole ER, Isbaine F, Hemptinne C de, Starr PA, Willie JT, et al. Multi-objective data-driven optimization for improving deep brain stimulation in Parkinson's disease. J Neural Eng 2021;18:046046. 10.1088/1741-2552/abf8ca.

[20]. Tinkhauser G, Pogosyan A, Debove I, Nowacki A, Shah SA, Seidel K, et al. Directional local field potentials: a tool to optimize deep brain stimulation. Mov Disord 2018;33:159–64. 10.1002/mds.27215. [PubMed: 29150884]

[21]. Broadway JM, Holtzheimer PE, Hilimire MR, Parks NA, DeVylder JE, Mayberg HS, et al. Frontal theta cordance predicts 6-month antidepressant response to subcallosal cingulate deep brain stimulation for treatment-resistant depression: a pilot study. Neuropsychopharmacology 2012;37:1764–72. 10.1038/npp.2012.23. [PubMed: 22414813]

[22]. Sun Y, Giacobbe P, Tang CW, Barr MS, Rajji T, Kennedy SH, et al. Deep brain stimulation modulates gamma oscillations and theta–gamma coupling in treatment resistant depression. Brain Stimul: Basic, Translational, and Clinical Research in Neuromodulation 2015;8:1033–42. 10.1016/j.brs.2015.06.010.

[23]. Quraan MA, Protzner AB, Daskalakis ZJ, Giacobbe P, Tang CW, Kennedy SH, et al. EEG power asymmetry and functional connectivity as a marker of treatment effectiveness in DBS surgery for depression. Neuropsychopharmacology 2014;39: 1270–81. 10.1038/npp.2013.330. [PubMed: 24285211]

[24]. McConnell GC, So RQ, Hilliard JD, Lopomo P, Grill WM. Effective deep brain stimulation suppresses low-frequency network oscillations in the basal ganglia by regularizing neural firing patterns. J Neurosci 2012;32:15657–68. 10.1523/JNEUROSCI.2824-12.2012. [PubMed: 23136407]

[25]. Baxter LR Jr, Schwartz JM, Phelps ME, Mazziotta JC, Guze BH, Selin CE, et al. Reduction of prefrontal cortex glucose metabolism common to three types of depression. Arch Gen Psychiatr 1989;46:243–50. 10.1001/archpsyc.1989.01810030049007. [PubMed: 2784046]

[26]. Jung J, Kang J, Won E, Nam K, Lee M-S, Tae WS, et al. Impact of lingual gyrus volume on antidepressant response and neurocognitive functions in Major Depressive Disorder: a voxel-based morphometry study. J Affect Disord 2014;169: 179–87. 10.1016/j.jad.2014.08.018. [PubMed: 25200096]

[27]. Kim SM, Park SY, Kim YI, Son YD, Chung U-S, Min KJ, et al. Affective network and default mode network in depressive adolescents with disruptive behaviors. Neuropsychiatric Dis Treat 2015;12:49–56. 10.2147/NDT.S95541.

[28]. Scalabrini A, Vai B, Poletti S, Damiani S, Mucci C, Colombo C, et al. All roads lead to the default-mode network—global source of DMN abnormalities in major depressive disorder. Neuropsychopharmacology 2020;45:2058–69. 10.1038/s41386-020-0785-x. [PubMed: 32740651]

[29]. Suh JS, Schneider MA, Minuzzi L, MacQueen GM, Strother SC, Kennedy SH, et al. Cortical thickness in major depressive disorder: a systematic review and meta-analysis. Prog Neuro Psychopharmacol Biol Psychiatr 2019;88:287–302. 10.1016/j.pnpbp.2018.08.008.

[30]. Xiao J, Provenza NR, Asfouri J, Myers J, Mathura RK, Metzger B, et al. Decoding depression severity from intracranial neural activity. Biol Psychiatr 2023. 10.1016/j.biopsych.2023.01.020.

[31]. Grimm S, Boesiger P, Beck J, Schuepbach D, Bermpohl F, Walter M, et al. Altered negative BOLD responses in the default-mode network during emotion processing in depressed subjects. Neuropsychopharmacology 2009;34:932–43. 10.1038/npp.2008.81. [PubMed: 18536699]

[32]. Runia N, Yücel DE, Lok A, de Jong K, Denys DAJP, van Wingen GA, et al. The neurobiology of treatment-resistant depression: a systematic review of neuroimaging studies. Neurosci Biobehav Rev 2022;132:433–48. 10.1016/j.neubiorev.2021.12.008. [PubMed: 34890601]

[33]. Manning KJ, Steffens DC. Chapter 11 - systems neuroscience in late-life depression. In: Frodl T, editor. Systems neuroscience in depression. San Diego: Academic Press; 2016. p. 325–40. 10.1016/B978-0-12-802456-0.00011-X.

[34]. Li H, Goldin P, Siegle GJ. 1.08 - neuroscience for clinicians: translational clinical neuroscience to inspire clinical practice and research. In: Asmundson GJG, editor. Comprehensive clinical psychology. second ed. Oxford: Elsevier; 2022. p. 145–67. 10.1016/B978-0-12-818697-8.00190-4.

[35]. Satpute AB, Lindquist KA. The default mode network's role in discrete emotion. Trends Cognit Sci 2019;23:851–64. 10.1016/j.tics.2019.07.003. [PubMed: 31427147]

[36]. Todd TP, Fournier DI, Bucci DJ. Retrosplenial cortex and its role in cue-specific learning and memory. Neurosci Biobehav Rev 2019;107:713–28. 10.1016/j.neubiorev.2019.04.016. [PubMed: 31055014]

[37]. Berman MG, Peltier S, Nee DE, Kross E, Deldin PJ, Jonides J. Depression, rumination and the default network. Soc Cognit Affect Neurosci 2011;6:548–55. 10.1093/scan/nsq080. [PubMed: 20855296]

[38]. Maguire E. The retrosplenial contribution to human navigation: a review of lesion and neuroimaging findings. Scand J Psychol 2001;42:225–38. 10.1111/1467-9450.00233. [PubMed: 11501737]

[39]. Mitchell AS, Czajkowski R, Zhang N, Jeffery K, Nelson AJD. Retrosplenial cortex and its role in spatial cognition. Brain and Neuroscience Advances 2018;2: 2398212818757098. 10.1177/2398212818757098.

[40]. Maddock RJ. The retrosplenial cortex and emotion: new insights from functional neuroimaging of the human brain. Trends Neurosci 1999;22:310–6. 10.1016/S0166-2236(98)01374-5. [PubMed: 10370255]

[41]. Corcoran KA, Frick BJ, Radulovic J, Kay LM. Analysis of coherent activity between retrosplenial cortex, hippocampus, thalamus, and anterior cingulate cortex during retrieval of recent and remote context fear memory. Neurobiol Learn Mem 2016; 127:93–101. 10.1016/j.nlm.2015.11.019. [PubMed: 26691782]

[42]. Cato MA, Crosson B, Gökçay D, Soltysik D, Wierenga C, Gopinath K, et al. Processing words with emotional connotation: an fMRI study of time course and laterality in rostral frontal and retrosplenial cortices. J Cognit Neurosci 2004;16: 167–77. 10.1162/089892904322984481. [PubMed: 15068589]

[43]. Li G, Zhang S, Le TM, Tang X, Li C-SR. Neural responses to negative facial emotions: sex differences in the correlates of individual anger and fear traits. Neuroimage 2020;221:117171. 10.1016/j.neuroimage.2020.117171. [PubMed: 32682098]

[44]. Bowman AD, Griffis JC, Visscher KM, Dobbins AC, Gawne TJ, DiFrancesco MW, et al. Relationship between alpha rhythm and the default mode network: an EEG-fMRI study. J Clin Neurophysiol 2017;34:527–33. 10.1097/WNP.0000000000000411. [PubMed: 28914659]

[45]. Flasbeck V, Enzi B, Brüne M. Enhanced processing of painful emotions in patients with borderline personality disorder: a functional magnetic resonance imaging study. Front Psychiatr 2019;10.

[46]. Minoshima S, Giordani B, Berent S, Frey KA, Foster NL, Kuhl DE. Metabolic reduction in the posterior cingulate cortex in very early Alzheimer's disease. Ann Neurol 1997;42:85–94. 10.1002/ana.410420114. [PubMed: 9225689]

[47]. Posner J, Song I, Lee S, Rodriguez CI, Moore H, Marsh R, et al. Increased functional connectivity between the default mode and salience networks in unmedicated adults with obsessive-compulsive disorder. Hum Brain Mapp 2016;38:678–87. 10.1002/hbm.23408. [PubMed: 27659299]

[48]. Gentili C, Ricciardi E, Gobbini MI, Santarelli MF, Haxby JV, Pietrini P, et al. Beyond amygdala: default Mode Network activity differs between patients with Social Phobia and healthy controls. Brain Res Bull 2009;79:409–13. 10.1016/j.brainresbull.2009.02.002. [PubMed: 19559343]

[49]. Andreasen NC, O'Leary DS, Flaum M, Nopoulos P, Watkins GL, Ponto LLB, et al. Hypofrontality in schizophrenia: distributed dysfunctional circuits in neuroleptic-naïve patients. Lancet 1997;349:1730–4. 10.1016/S0140-6736(96)08258-X. [PubMed: 9193383]

[50]. Ho AP, Gillin JC, Buchsbaum MS, Wu JC, Abel L, Bunney WE Jr. Brain glucose metabolism during non—rapid eye movement sleep in major depression: a positron emission tomography study. Arch Gen Psychiatr 1996;53:645–52. 10.1001/archpsyc.1996.01830070095014. [PubMed: 8660131]

[51]. Wei G-X, Ge L, Chen L-Z, Cao B, Zhang X. Structural abnormalities of cingulate cortex in patients with first-episode drug-naïve schizophrenia comorbid with depressive symptoms. Hum Brain Mapp 2021;42:1617–25. 10.1002/hbm.25315. [PubMed: 33296139]

[52]. Miller EK, Cohen JD. An integrative theory of prefrontal cortex function. Annu Rev Neurosci 2001;24:167–202. 10.1146/annurev.neuro.24.1.167. [PubMed: 11283309]

[53]. Seeley WW, Menon V, Schatzberg AF, Keller J, Glover GH, Kenna H, et al. Dissociable intrinsic connectivity networks for salience processing and executive control. J Neurosci 2007;27:2349–56. 10.1523/JNEUROSCI.5587-06.2007. [PubMed: 17329432]

[54]. Fox MD, Snyder AZ, Vincent JL, Corbetta M, Van Essen DC, Raichle ME. The human brain is intrinsically organized into dynamic, anticorrelated functional networks. Proc Natl Acad Sci USA 2005;102:9673–8. 10.1073/pnas.0504136102. [PubMed: 15976020]

[55]. Chen C-MA, Stanford AD, Mao X, Abi-Dargham A, Shungu DC, Lisanby SH, et al. GABA level, gamma oscillation, and working memory performance in schizophrenia. Neuroimage: Clinic 2014;4:531–9. 10.1016/j.nicl.2014.03.007.

[56]. Webb CA, Dillon DG, Pechtel P, Goer FK, Murray L, Huys QJ, et al. Neural correlates of three promising endophenotypes of depression: evidence from the EMBARC study. Neuropsychopharmacology 2016;41:454–63. 10.1038/npp.2015.165. [PubMed: 26068725]

[57]. Kito S, Pascual-Marqui RD, Hasegawa T, Koga Y. High-frequency left prefrontal transcranial magnetic stimulation modulates resting EEG functional connectivity for gamma band between the left dorsolateral prefrontal cortex and precuneus in depression. Brain Stimul: Basic, Translational, and Clinical Research in Neuromodulation 2014;7:145–6. 10.1016/j.brs.2013.09.006.

[58]. Pascual-Leone A, Rubio B, Pallardó F, Catalá MD. Rapid-rate transcranial magnetic stimulation of left dorsolateral prefrontal cortex in drug-resistant depression. Lancet 1996;348:233–7. 10.1016/S0140-6736(96)01219-6. [PubMed: 8684201]

[59]. Kanno M, Matsumoto M, Togashi H, Yoshioka M, Mano Y. Effects of acute repetitive transcranial magnetic stimulation on dopamine release in the rat dorsolateral striatum. J Neurol Sci 2004;217:73–81. 10.1016/j.jns.2003.08.013. [PubMed: 14675613]

[60]. Avissar M, Powell F, Ilieva I, Respino M, Gunning FM, Liston C, et al. Functional connectivity of the left DLPFC to striatum predicts treatment response of depression to TMS. Brain Stimul: Basic, Translational, and Clinical Research in Neuromodulation 2017;10:919–25. 10.1016/j.brs.2017.07.002.

[61]. Luo Q, Chen J, Li Y, Wu Z, Lin X, Yao J, et al. Altered regional brain activity and functional connectivity patterns in major depressive disorder: a function of childhood trauma or diagnosis? J Psychiatr Res 2022;147:237–47. 10.1016/j.jpsychires.2022.01.038. [PubMed: 35066292]

[62]. Respino M, Jaywant A, Kuceyeski A, Victoria LW, Hoptman MJ, Scult MA, et al. The impact of white matter hyperintensities on the structural connectome in late-life depression: relationship to executive functions. Neuroimage: Clinic 2019;23: 101852. 10.1016/j.nicl.2019.101852.

[63]. Buyukdura JS, McClintock SM, Croarkin PE. Psychomotor retardation in depression: biological underpinnings, measurement, and treatment. Prog Neuro-Psychopharmacol Biol Psychiatry 2011;35:395–409. 10.1016/j.pnpbp.2010.10.019.

[64]. Banker L, Tadi P. Neuroanatomy, precentral gyrus. StatPearls. Treasure Island (FL): StatPearls Publishing; 2022.

[65]. Hamani C, Mayberg H, Stone S, Laxton A, Haber S, Lozano AM. The subcallosal cingulate gyrus in the context of major depression. Biol Psychiatr 2011;69:301–8. 10.1016/j.biopsych.2010.09.034.

[66]. Na K-S, Won E, Kang J, Chang HS, Yoon H-K, Tae WS, et al. Brain-derived neurotrophic factor promoter methylation and cortical thickness in recurrent major depressive disorder. Sci Rep 2016;6:21089. 10.1038/srep21089. [PubMed: 26876488]

[67]. Spironelli C, Maffei A, Romeo Z, Piazzon G, Padovan G, Magnolfi G, et al. Evidence of language-related left hypofrontality in Major Depression: an EEG Beta band study. Sci Rep 2020;10:8166. 10.1038/s41598-020-65168-w. [PubMed: 32424130]

[68]. Guha A, Spielberg JM, Lake J, Popov T, Heller W, Yee CM, et al. Effective connectivity between Broca's area and amygdala as a mechanism of top-down control in worry. Clin Psychol Sci 2020;8:84–98. 10.1177/2167702619867098. [PubMed: 32983628]

[69]. Isenberg N, Silbersweig D, Engelien A, Emmerich S, Malavade K, Beattie B, et al. Linguistic threat activates the human amygdala. Proc Natl Acad Sci USA 1999;96: 10456–9. 10.1073/pnas.96.18.10456. [PubMed: 10468630]

[70]. Wang Y, Jiang P, Tang S, Lu L, Bu X, Zhang L, et al. Left superior temporal sulcus morphometry mediates the impact of anxiety and depressive symptoms on sleep quality in healthy adults. Soc Cognit Affect Neurosci 2021;16:492–501. 10.1093/scan/nsab012. [PubMed: 33512508]

[71]. Zhu Z, Hubbard E, Guo X, Barbosa DAN, Popal AM, Cai C, et al. A connectomic analysis of deep brain stimulation for treatment-resistant depression. Brain Stimul 2021;14:1226–33. 10.1016/j.brs.2021.08.010. [PubMed: 34400379]

[72]. Riva-Posse P, Choi KS, Holtzheimer PE, McIntyre CC, Gross RE, Chaturvedi A, et al. Defining critical white matter pathways mediating successful subcallosal cingulate deep brain stimulation for treatment-resistant depression. Biol Psychiatr 2014;76: 963–9. 10.1016/j.biopsych.2014.03.029.

Significance statement

Deep brain stimulation (DBS) is a highly effective treatment for movement disorders, but of mixed efficacy in psychiatric disorders, such as treatment-resistant depression (TRD). Since DBS in TRD is a newer and more experimental indication, stimulation programming procedures are less optimized. In DBS for TRD, stimulation optimization may require months of clinical observation to evaluate a particular setting configuration, whereas in stimulation effects in movement disorders can be observed within seconds-minutes. As such, we sought to identify electrophysiological biomarker candidates which may provide an alternative, acutely assessable information source (seconds-minutes per evaluation) for DBS optimization in TRD.

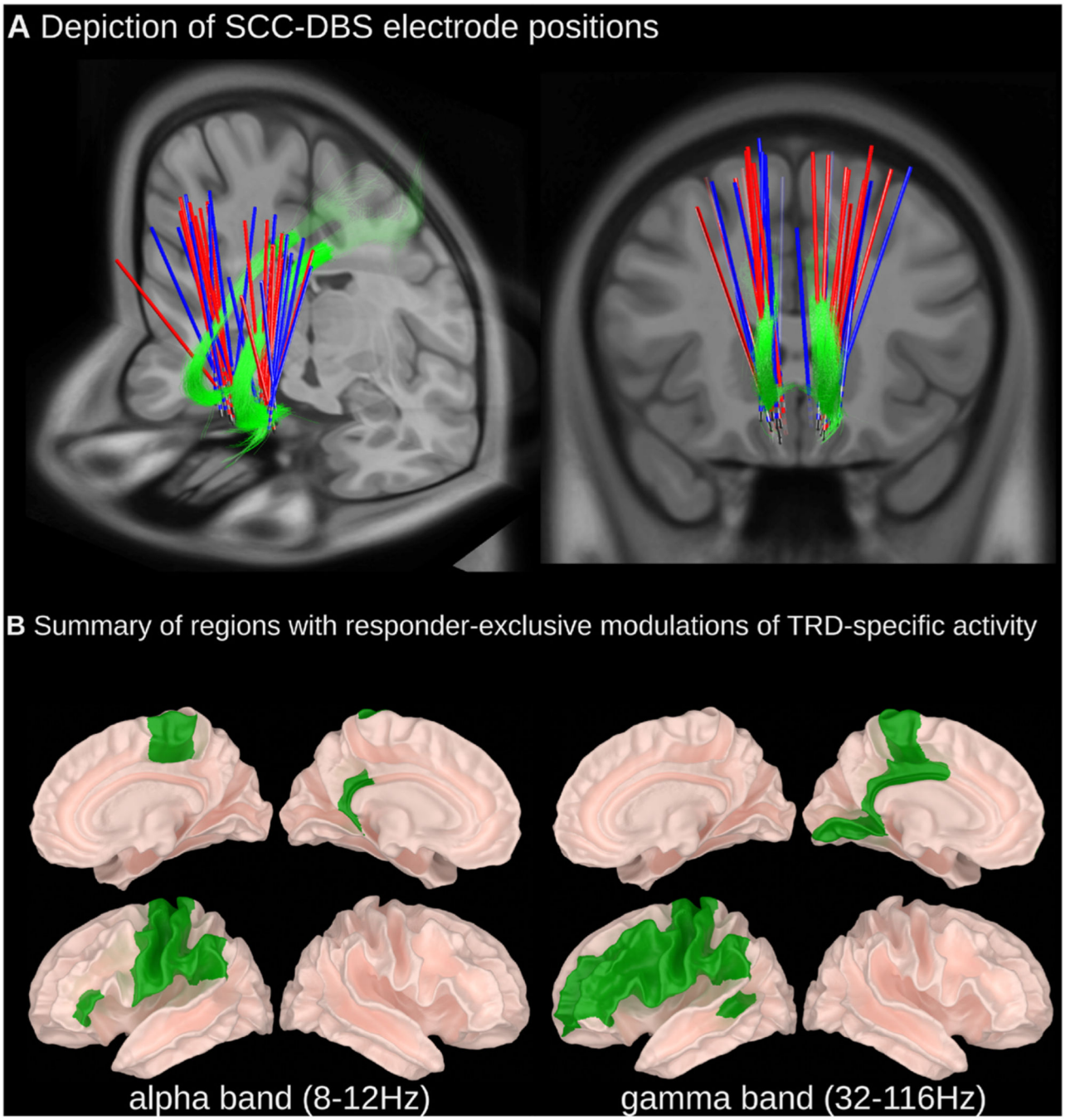

Fig. 1. (A) Depiction of SCC-DBS electrode positions and (B) summary of regions with responder-specific modulations of TRD-specific activity.

(A) DBS lead positions are shown for responder (blue) and non-responder (red) subgroups relative to the cingulum bundle (green). Lead localization was done using LeadDBS (detailed methods available within Supplementary Material). **(B)** A depictive summary of brain regions that expressed statistically significant differences in relative oscillatory power in people with TRD (SCC-DBS OFF) compared to HCs wherein TRD-specific differences were counteracted by SCC-DBS ON in responders only. Detailed statistical

results and depictions on a region-by-region basis are provided in the subsequent figures. (For interpretation of the references to colour in this figure legend, the reader is referred to the Web version of this article.)

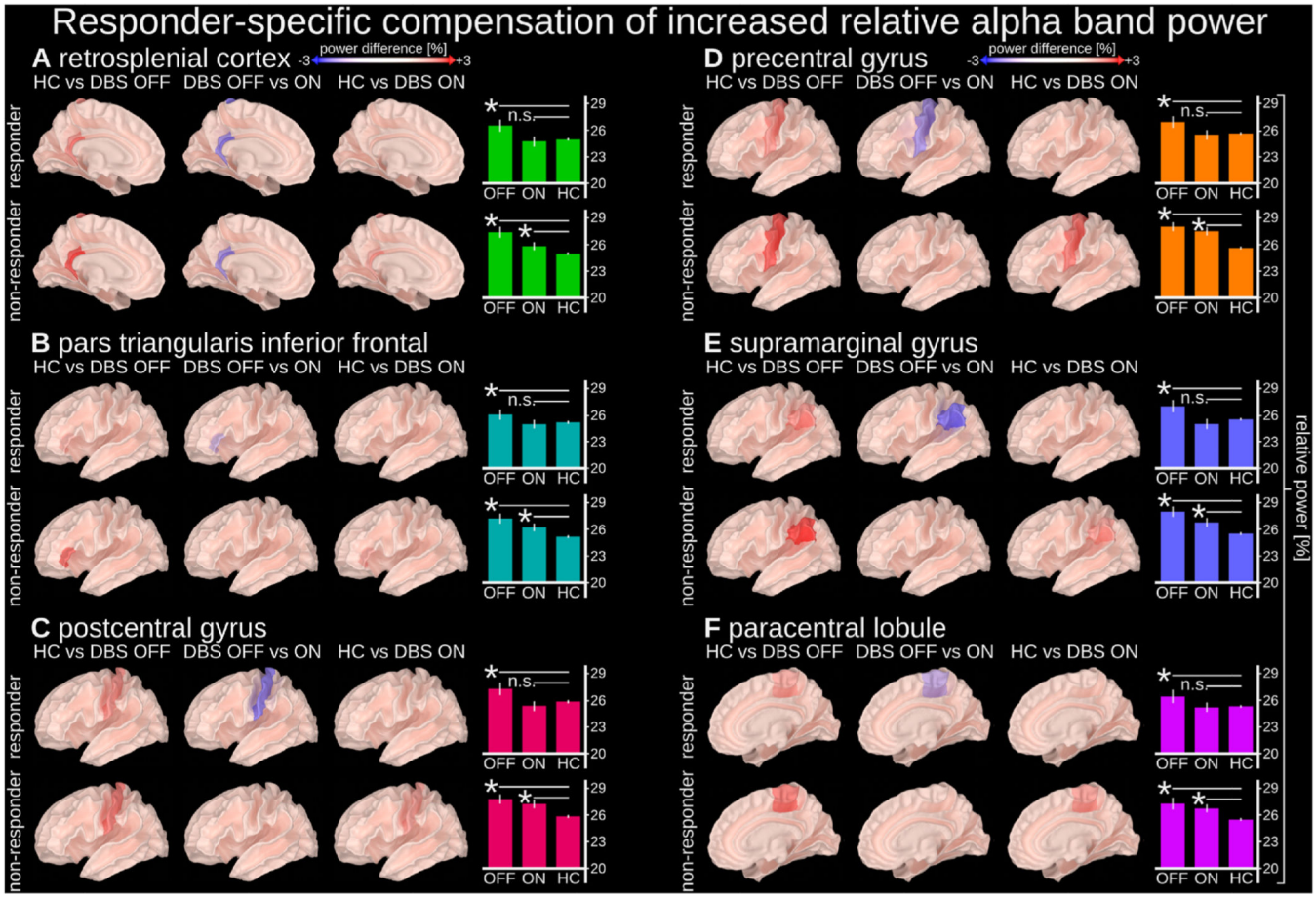

Fig. 2. Responder-specific compensation of increased relative alpha power.

Relative alpha power (8–12 Hz) in the highlighted regions was increased in people with depression (both responders and non-responders with SCC-DBS OFF) compared to HCs, but compensated by SCC-DBS in responders only (i.e., statistically indistinguishable from HCs with SCC-DBS ON). Relative alpha power was measured as the ratio between the alpha (8–12 Hz) sub-band and broadband (2–116 Hz) power. Normalization Compensation of increased relative alpha power was observed in the left (A) retrosplenial cortex, (B) inferior frontal cortex, (C) postcentral gyrus, (D) precentral gyrus, (E) supramarginal gyrus, and (F) right paracentral lobule. The cortical surface images depict relative alpha power differences between implicated states. The bar graphs depict the absolute values of the relative power within individual states (with statistical comparisons in relation to HC). DBS OFF n = 16; DBS ON = 14; HC n = 25.

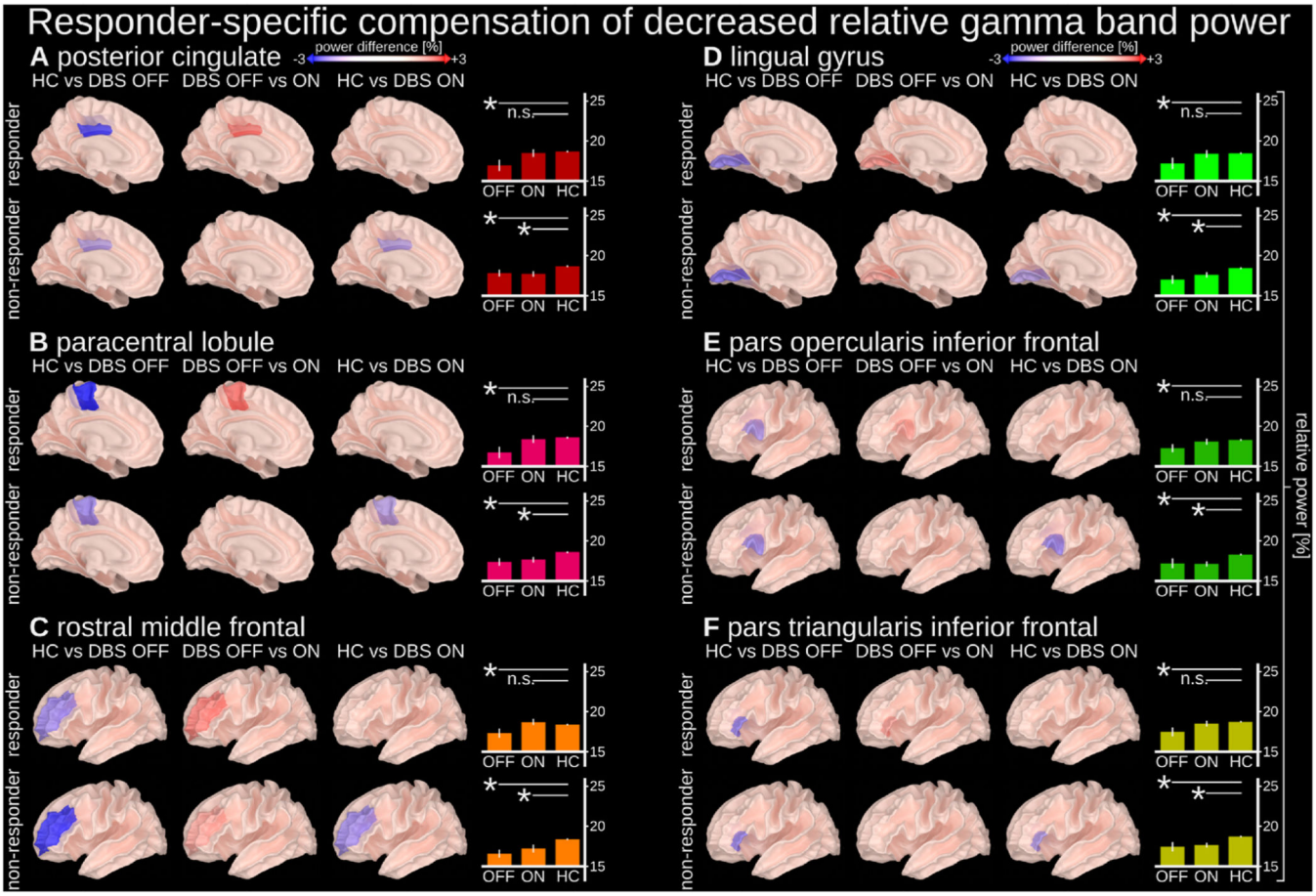

Fig. 3. Responder-specific compensation of decreased gamma band relative power.

Relative gamma power (32–116 Hz) in the highlighted regions was decreased in people with depression (both responders and non-responders with SCC-DBS OFF) compared to HCs, but compensated by SCC-DBS ON in responders only (i.e., statistically indistinguishable from HCs with SCC-DBS ON). Relative gamma power was measured as the ratio between the gamma (32–116 Hz) sub-band and broadband (2–116 Hz) power. Compensation of decreased relative gamma power was observed in the left (A) posterior cingulate, (B) paracentral lobule, (C) rostral middle frontal cortex, (D) lingual gyrus, (E) inferior frontal cortex pars opercularis, and (F) inferior frontal cortex pars triangularis. The cortical surface images depict relative gamma power differences between implicated states. The bar graphs depict the absolute values of the relative power within individual states (with statistical comparisons in relation to HC). DBS OFF n = 16; DBS ON = 14; HC n = 25.

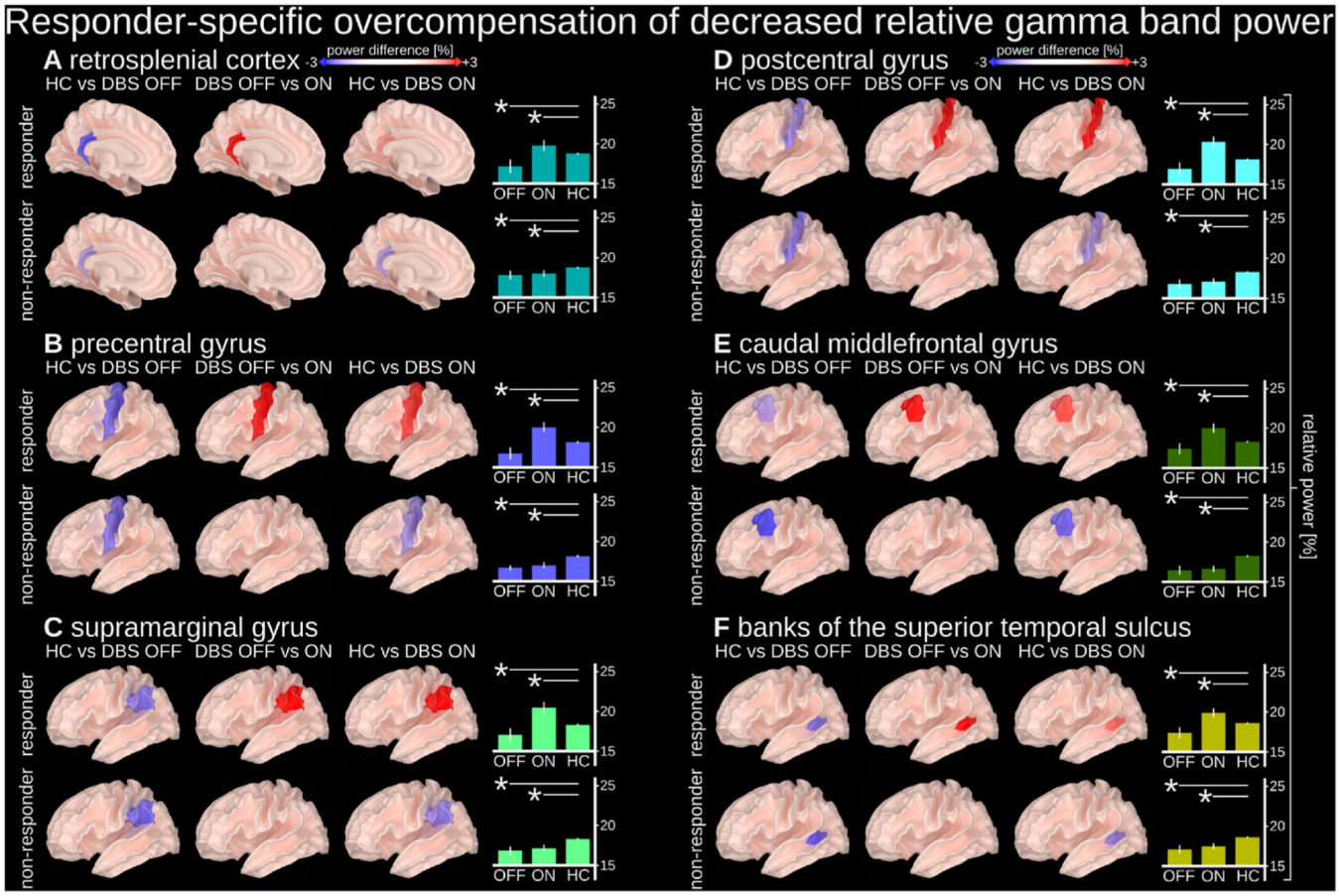

Fig. 4. Responder-specific overcompensation of decreased relative gamma band power.

Relative gamma power (32–116 Hz) in the highlighted regions was found to be decreased in people with depression (both responders and non-responders with DBS OFF) compared to HCs, but reversed by SCC-DBS ON in responders only (i.e., hypoactivity became hyperactivity). Relative gamma power was measured as the ratio between a gamma (32–116 Hz) sub-band and broadband (2–116 Hz) power. Overcompensation of decreased relative gamma power was observed in the left (A) retrosplenial cortex, (B) precentral gyrus, (C) supramarginal gyrus, (D) postcentral gyrus, (E) caudal middle frontal cortex, and (F) banks of the superior temporal sulcus. The cortical surface images depict relative gamma power differences between implicated states. The bar graphs depict the absolute values of the relative power within individual states (with statistical comparisons in relation to HC). DBS OFF n = 16; DBS ON = 14; HC n = 25.

Fig. 5. Investigation of the effects of stimulation amplitude and frequency.

(A) Bilateral stimulation at 130 Hz/1.5 mA was associated with undercompensated activity in non-responders and compensated and/or overcompensated activity in responders; this column represents the statistical summary of Figs. 2–4 (B) Unilateral stimulation at 130 Hz/1.5 mA was associated with generally undercompensated activity in both responders and non-responders in both alpha and gamma frequency bands; this condition is intended to serve as a new baseline to investigate the effects of stimulation amplitude and frequency. (C) Unilateral stimulation at 130 Hz using a higher amplitude of 3.0 mA (instead of

1.5 mA) led to strengthened modulatory effects (i.e., less undercompensated nodes). (D) Unilateral stimulation at 1.5 mA using a lower stimulation frequency of 20 Hz (instead of 130 Hz) led to even stronger modulatory effects (i.e., less undercompensated nodes and more overcompensated nodes). R = responders; NR = non-responders. Detailed statistical depictions are available in Supplementary Figs. 5 and 6. DBS OFF n = 16; DBS ON (A) n = 14, (B) n = 15, (C) n = 14, (D) n = 14; HC n = 25.

Table 1

Clinical characteristics and therapeutic DBS settings of TRD participants.

Subject	Age of MDD onset	MDD duration (y)	MDD features		DBS duration (y)	HAMD-17 score		% Improvement with SCC-DBS (%)[b]	Responder status	Therapeutic DBS settings			
			Melancholic	Anxious		SCC-DBS OFF	SCC-DBS ON			Bilateral contact configuration	Amplitude (mA)	Pulse width (μs)	Frequency (Hz)
						Pre-operative score	*12-month post-operative score*						
1	21	4	no	yes	0.1	26	3	88.5	Responder	C+1−	3.5	91	130
2	30	21	yes	yes	0.7	30	13	56.7	Responder	C+1−	4.5	91	130
3	22	27	no	yes	9.3	31	15	51.6	Responder	*a*	*a*	*a*	*a*
4	37	18	yes	yes	2.3	30	14	53.3	Responder	C+1−2−	6.5	91	130
5	16	30	yes	yes	0.8	23	16	30.4	Non-responder	C+1−	5.5	91	130
6	15	37	yes	no	10.9	24	11	54.2	Responder	C+1−	5.5	60	130
7	17	29	yes	no	0.9	22	24	− 9.1	Non-responder	C+1−2−	4.5	91	130
8	19	33	no	yes	5.6	26	14	46.2	Non-responder	C+2−	9	87	130
9	16	32	yes	yes	9.9	20	17	15	Non-responder	C+1−	6	90	130
10	22	24	no	yes	4.5	26	28	−7.7	Non-responder	1+/2−	7.5	91	130
11	12	34	yes	no	2.0	22	23	−4.5	Non-responder	C+3−	7.5	91	130
12	19	16	no	yes	1.8	22	5	77.3	Responder	C+2−	11	91	130
13	26	15	no	yes	4.0	23	6	73.9	Responder	C+1−	7	91	130
14	31	22	*a*	*a*	8.9	25	13	48	Non-responder	C+1−	7	87	130
15	13	22	yes	yes	4.1	23	20	13	Non-responder	C+1−2−	7	91	130

[a] Depressive symptom improvement represents the percent change in HAMD-17 score between SCC-DBS OFF (pre-operative score) and ON (12-month post-operative score). Percent improvement is calculated as [(DBS ON - DBS OFF)/DBS OFF] x (—100). Positive values represent an improvement in symptoms (lower HAMD-17 score) with SCC-DBS; negative values represent a worsening in symptoms (higher HAMD-17 score) with SCC-DBS.

[**] 60 μs pulse width used for patient 6. DBS, deep brain stimulation; HAMD-17, 17-item Hamilton Depression Rating Scale; SCC, subcallosal cingula.